Int. J. Electrochem. Sci., 6 **(2011)** 1331 - 1341

International Journal of
ELECTROCHEMICAL
SCIENCE
www.electrochemsci.org

Electrochemical Fabrication of AuRh Nanoparticles and their Electroanalytical Applications

Ching-Yi Cheng, Soundappan Thiagarajan, Shen-Ming Chen[*]

Electroanalysis and Bioelectrochemistry Lab, Department of Chemical Engineering and Biotechnology, National Taipei University of Technology, No.1, Section 3, Chung-Hsiao East Road, Taipei 106, Taiwan (ROC).
[*]E-mail: smchen78@ms15.hinet.net

Received: 13 November 2010 / *Accepted:* 29 March 2011 / *Published:* 1 May 2011

Fabrication of nano AuRh nanoparticles film modified GCE has been successfully carried out using 0.5 M H_2SO_4 as electrolyte. AuRh nanoparticles film modified GCE electrodes examined using atomic force microscopy (AFM), SEM and X-ray diffraction studies (XRD). Fabricated nano AuRh particles average diameter have been found as 55 nm. The nano AuRh nanoparticles modified GCE successfully reduces the over potential and shows the well defined oxidation peaks for the detection of ascorbic acid (AA), dopamine (DA), reduction of bromate and simultaneous determination of AA and dopamine (DA) (in pH 7.0 phosphate buffer solution (PBS)) using cyclic voltammetry (CV) and linear sweep voltammetry (LSV). Also, the AuRh nanoparticles modified GCE exhibits good linear range for the simultaneous detection of AA and DA in lab and real samples using LSV.

Keywords: AuRh nanoparticles, Cyclic voltammetry, Ascorbic acid, Dopamine, Bromate.

1. INTRODUCTION

Successful fabrication of metal nanoparticles using various electrochemical methods for the electrode modification process is the current trend in electroanalytical chemistry. Electrodeposited metal nanoparticles modified electrodes possess interesting electrochemical activities for the detection of various types of chemical compounds and biomolecules [1]. Not only limited to single metal nanoparticles, bimetallic nanoparticles also hold the special electrochemical behavior for the detection of important compounds [2]. Especially, noble metal nanoparticles will be more favorable and much utilized for the electrode modification process [3,4]. Particularly, electrochemical synthesis of rhodium (Rh) nanoparticles leads the pathway for the fabrication of new type of nano film modified electrodes.

Various methods have been employed for the fabrication of Rh nanoparticles. For example electrochemical synthesis [5], preparation and characterization of rhodium nanostructures through the evolution of microgalvanic cells and their enhanced electrocatalytic activity for formaldehyde oxidation [6], dendrimer-rhodium nanoparticle modified glassy carbon electrode (GCE) for amperometric detection of hydrogen peroxide [7], one-step synthesis of size-tunable rhodium nanoparticles on carbon nanotubes [8] were reported.

Not only limited to Rh nanoparticles, Rh based bimetallic nanoparticles also fabricated and applied for the various types of applications. Few examples were, preparation of Pt/Rh bimetallic colloidal particles in polymer solutions using borohydride-reduction [9], Rh-Pt bimetallic catalysts: synthesis, characterization, and catalysis [10], microwave synthesis of bimetallic nanoalloys and CO Oxidation [11], tuning of Catalytic CO Oxidation by Changing composition of Rh-Pt bimetallic nanoparticles [12], electrocatalysis of ethanol oxidation on Pt monolayers deposited on carbon-supported Ru and Rh nanoparticles [13], PtRh alloy nanoparticle electrocatalysts for oxygen reduction for use in direct methanol fuel cells [14] and simultaneous photo deposition of rhodium–chromium nanoparticles on a semiconductor powder: structural characterization and application to photocatalytic overall water splitting were reported [15].

The above mentioned research reports clearly shows the possibilities of the Rh and Rh combined nano metallic materials fabrication and their potential applications. Recently various types of nanomaterials modified electrodes have been reported for the detection and determination of AA, DA and UA [16-18]. Here, in this report we have attempted to fabricate the AuRh nanoparticles using cyclic voltammetry (CV). CV has been employed for the fabrication of AuRh nanoparticles modified GCE. AuRh nanoparticles modified GCE has been employed for the scanning electron microscopy (SEM) and atomic force microscopy (AFM) and electrochemical impedance spectroscopic (EIS) analysis. Fabricated AuRh nanoparticles modified GCE exhibits very good electrochemical response in pH 7.0 PBS solutions. Further the AuRh nanoparticles modified GCE has been successfully employed for the simultaneous detection of AA and DA in pH 7.0 PBS using CV and linear sweep voltammetry (LSV). Also, the AuRh nanoparticles modified GCE detects the electrochemical reduction signals of bromate, respectively.

2. MATERIALS AND METHODS

2.1. Reagents

Dopamine (DA), ascorbic acid (AA) and $KBrO_3$, were purchased from Sigma-Aldrich (USA). Rhodium (III) chloride hydrate (38-41 % Rh), potassium tetrachloro aurate (III) hydrate (98 %) was purchased from Strem Chemicals (USA). All other chemicals (Merck) used were of analytical grade (99 %). Double distilled deionized water was used to prepare all the solutions. A phosphate buffer solution (PBS) of pH 7.0 was prepared using Na_2HPO_4 (0.05 mol l^{-1}) and NaH_2PO_4 (0.05 mol l^{-1}). Pure nitrogen was passed through all the experimental solutions.

2.2. Apparatus

All electrochemical experiments were performed using CHI 410a potentiostat (CH Instruments,

USA). The BAS GCE (φ = 0.3 cm in diameter, exposed geometric surface area 0.07 cm^2, Bioanalytical Systems, Inc., USA) was used. A conventional three-electrode system was used which consists of an Ag/AgCl (saturated KCl) as a reference, bare or nano AuRh particles modified GCE as working and platinum wire as counter electrode. Electrochemical impedance studies (EIS) were performed using ZAHNER impedance analyzer (Germany). The AFM images were recorded with multimode scanning probe microscope (Being Nano-Instruments CSPM-4000, China). Scanning electron microscope (SEM) images were performed using HITACHI S-3000H (Japan).The XRD experiment was done using XPERT-PRO (PANalytical B.V., The Netherlands).

2.3. Fabrication of nano AuRh particles

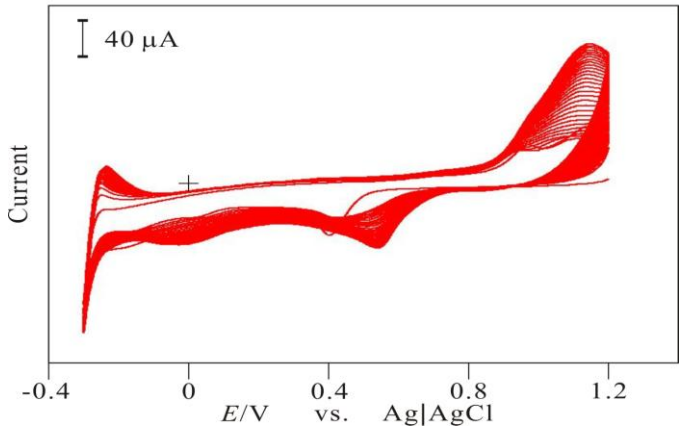

Figure 1. Consecutive cyclic voltammograms of AuRh nanoparticles deposition process on GCE using 0.5 M H_2SO_4 containing 1 × 10^{-3} M of $KAuCl_4.3H_2O$ and 3 × 10^{-4} M $RhCl_3$ in the potential range of 1.2 to -0.3 V (scan rate: 0.1 V/s) for thirty cycles.

Prior to the electrochemical deposition process, the GCE was well polished with the help of BAS polishing kit with aqueous slurries of alumina powder (0.05 μm), rinsed and ultrasonicated in double distilled deionized water. The pretreated GCE was immersed in 0.5 M H_2SO_4 containing 1 × 10^{-3}M $KAuCl_4$ and 3 × 10^{-4} M $RhCl_3$ and the potential cycling has been applied between 1.2 and -0.3 V at the scan rate of 0.1 V/s for thirty cycles (Figure-1). Further the AuRh nanoparticles modified GCE has been washed with deionized water and dried for 5 minutes and employed for the further electrochemical investigations.

3. RESULTS AND DISCUSSION

3.1. Characterization of AuRh nanoparticles

The electrodeposited AuRh nanoparticles modified GCE has been examined using SEM and

AFM techniques (Fig. 2). Fig. 2(A), (B) and (C) shows the SEM images of the AuRh nanoparticles modified GCE. From the Fig. 2(A), (B) and (C) (different magnifications), we can see the existence of AuRh nanoparticles in the obvious manner in the average size range of 55 nm. During the electrochemical deposition process, the particles have been deposited as separate and group of nanoparticles. Therefore, the big sizes of particles found in the SEM analysis were the coagulation of small nanoparticles, respectively.

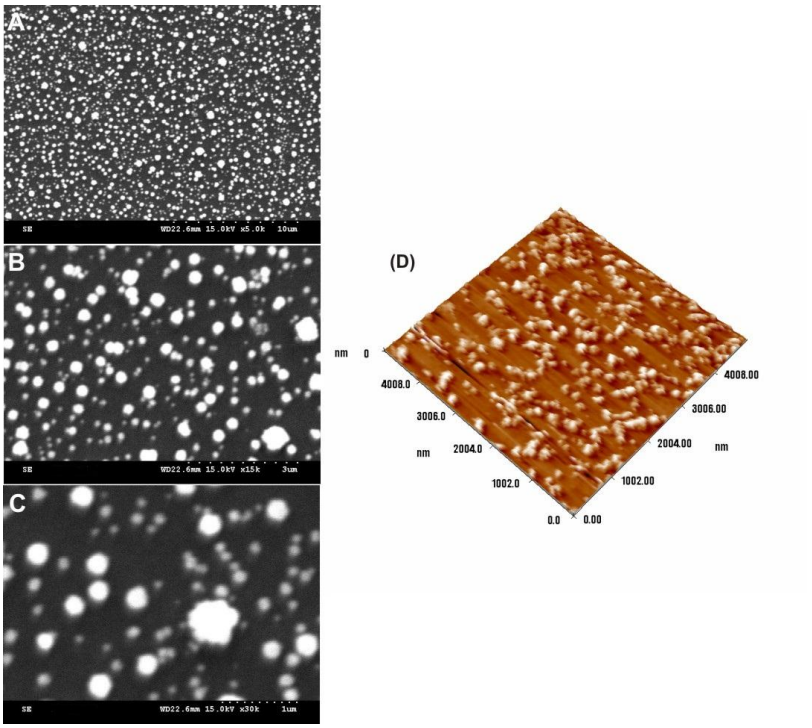

Figure 2. SEM images (A, B and C (Magnification: ×5k, ×15k and ×30k) of nano AuRh nanoparticles modified GCE. (D) AFM three dimensional view of electrodeposited nano AuRh nanoparticles modified GCE.

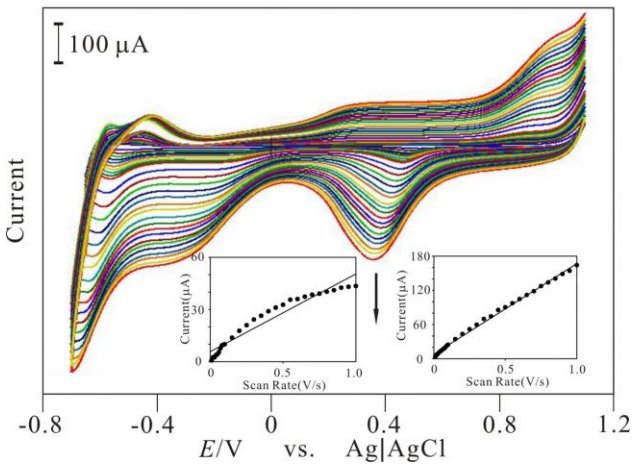

Figure 3. Different scan rate studies of AuRh nanoparticles modified GCE in pH 7.0 PBS. Scan rate in the range of 0.01 ~ 1 V/s. Inset shows the plot of cathodic peak currents of Au (0.35 V) and Rh (-0.27 V) vs. scan rate.

The AFM tapping mode has been employed for the analysis of AuRh nanoparticles modified GCE. Fig. 2(D) shows the three dimensional magnified view of the AuRh nanoparticles modified GCE. Here the total number of electrodeposited AuRh nanoparticles particles found within the 5010 × 5010 nm surface area was 509. Based on the AFM analysis, the average height of the AuRh nanoparticles have been found as 53.10 nm. Further the AuRh nanoparticles modified GCE's surface roughness average has been found as 23.8 nm.

Further, the surface skewness and kurtosis value have been found as 0.97 and 3.86, respectively. Based on the SEM and AFM analysis the surface morphologies of the nano AuRh particles modified GCE has been clearly validated. Fig. 1 illustrates AuRh nanoparticles electrodeposition process on GCE using CV. The forward scan was started at 1.2 V and scanned towards the negative direction up to −0.3 V. It exhibits two peaks corresponding to reduction of Au at 0.54 V, Rh −0.006 V, and for hydrogen adsorption desorption at around −0.23 V. On subsequent cycles, all the peaks were found growing. This result indicates that during the cycling process, the deposition of Au and Rh particles takes place on GCE.

The influence of scan rate on the electrochemical response of AuRh nanoparticles modified GCE was investigated in pH 7.0 PBS (Fig-3). Cyclic voltammetry was performed for the different scan rate studies. Here the cathodic peak currents of Au (0.35 V) and Rh (-0.27 V) increases clearly with respect to the scan rate in the range of 0.01 to 1 V/s. Here we can easily distinguish the both separate cathodic peak currents for the Au and Rh, respectively. Also, for the increasing scan rates the corresponding peak currents increase shows that the film possess the surface controlled electrochemical behavior. At the same time, the corresponding cathodic peak currents become much broader in the higher scan rates. Further the inset of Fig. 3 shows the plots cathodic peak currents of Au (0.35 V) and Rh (-0.27 V) vs. scan rate. Here the corresponding linear regression equations for the Au and Rh reduction were found as I_{pc} (μA) = 158.88v (V/s) + 7.99, R^2 = 0.9961 and I_{pa} (μA) = 44.702v (V/s) + 5.75, R^2 = 0.936.

3.2. XRD and EIS analysis

XRD has been employed to validate the proposed AuRh nanoparticles electrodeposited ITO. Fig. 4 (A) shows the XRD patterns obtained for the AuRh nanoparticles on ITO surface. Five different and important characteristic peaks obtained for the electrodeposited nano AuRh particles. They are, 30.69 (220), 35.26 (222), 38.50 (111), 44.79 (331) and 50.90 (422). The remaining peaks pattern corresponds to the ITO surface. This five peaks (30.69 (220), 35.26 (222), 38.50 (111), 44.79 (331) and 50.90 (422)) validate the electrodeposited AuRh nanoparticles on the ITO surface. Finally, based on this XRD analysis the presence of AuRh nanoparticles has been confirmed.

The electrochemical activity of AuRh nanoparticles modified GCE has been examined using EIS technique. Impedance spectroscopy is an effective method to probe the features of surface modified electrodes. This study was employed to analyze detailed electrochemical activities of modified electrode with individual or mixed components. The complex impedance can be presented as a sum of the real, Z' (ω), and imaginary Z'' (ω), components that originate mainly from the resistance

and capacitance of the cell. From the shape of an impedance spectrum, the electron-transfer kinetics and diffusion characteristics can be extracted. The respective semicircle parameters correspond to the electron transfer resistance (R_{et}) and the double layer capacity (C_{dl}) nature of the modified electrode. Fig. 4(B) shows the Faradaic impedance spectra, presented as Nyquist plots (Z'' vs. Z') for the bare, AuRh, Rh and Au particles modified GCE.

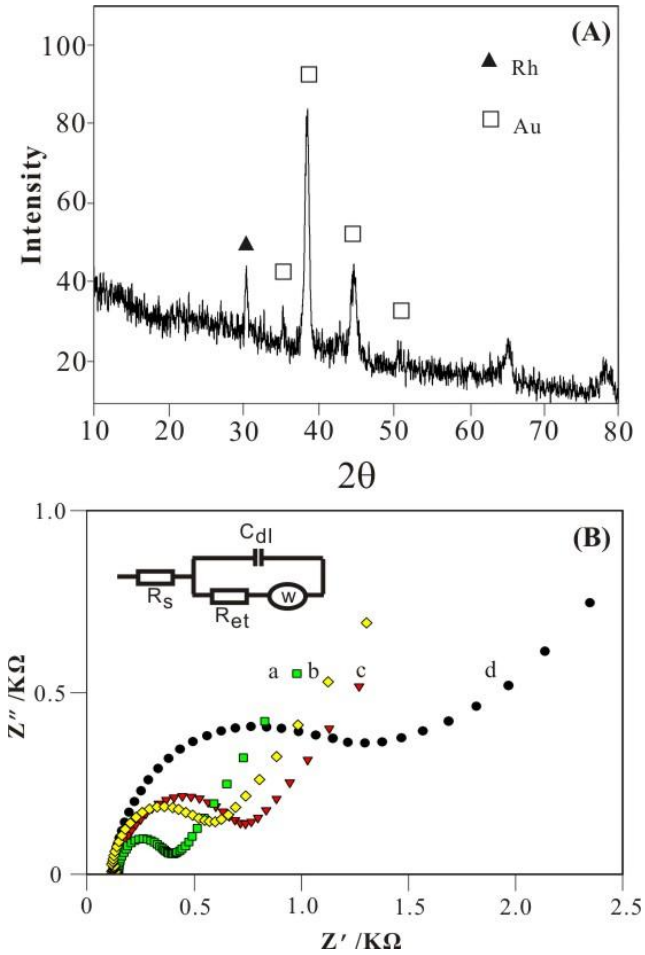

Figure 4. (A) XRD pattern of nano AuRh nanoparticles electrodeposited ITO. (B) Electrochemical impedance spectra curves of (a) bare (b) AuRh, (c) Rh (d) Au particles film modified GCE in pH 7.0 PBS containing 5×10^{-3} M $[Fe(CN)_6]^{-3/-4}$ (Amplitude: 5 mV).

The bare GCE exhibits with a small semi circle arc (R_{et} = 0.23 (Z'/KΩ)) represents the characteristics of diffusion limited electron-transfer process on the electrode surface. For the only Rh(curve c) and Au(curve d) film modified GCE shows like a semi circle arcs with the Ret values of 0.48 and 0.98 KΩ. At the same time, the AuRh nanoparticles modified GCE shows a small semi circle arc with the lower Ret value of 0.40 KΩ (curve b). This shows that the proposed AuRh particles modified GCE possess the lower electron transfer resistance behavior comparing with the other film modified electrodes. Here the lower R_{et} value (0.40 KΩ) obtained because of the bimetallic nature of the AuRh film modified GCE. Finally, these results clearly illustrate the electrochemical activities of the AuRh nanoparticles modified GCE, respectively.

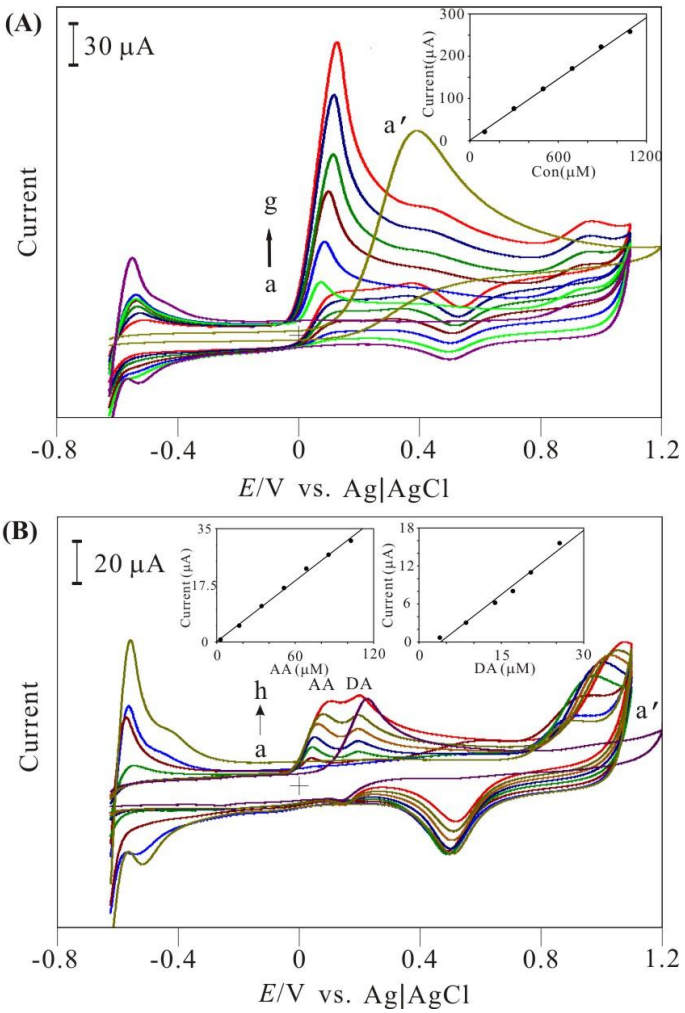

Figure 5. A) Cyclic voltammograms of AuRh nanoparticles modified GCE for the detection of AA in pH 7.0 PBS. AA concentrations were in the range of: (a-g) 0, 100, 299, 497, 695, 891 and 1088 µM, (a') bare GCE = 1088 µM, potential = 0.38 V (scan rate: 0.1 V/s). Inset shows the calibration plot of oxidation current vs. concentration of AA. (B) Cyclic voltammograms of AuRh nanoparticles modified GCE for the simultaneous detection of AA and DA in pH 7.0 PBS. AA concentrations were in the range of: (a-h) 0, 2.8, 17.1, 34.3, 51.4, 68.5, 85.5 and 102.6 µM, (a') bare GCE = 102.6 µM (0.22 V) (scan rate: 0.1 V/s). DA concentrations were in the range of: (a-h) 0, 0.71, 3.78, 8.56, 13.8, 17.1, 20.3 and 25.6 µM, (a') bare GCE = 25.6 µM (0.22 V)(scan rate: 0.1 V/s). Inset shows the calibration plots of current vs. concentration plots of AA and DA.

3.3. Electrocatalytic oxidation of AA at AuRh nanoparticles modified GCE

Figure 5(A) shows the cyclic voltammetric response of AuRh nanoparticles modified GCE for the detection of AA. As it can be seen in Fig. 5(A), a single oxidation peak at 0.07 V can be observed in the pH 7.0 PBS solution for the AA oxidation reaction. Further it can be noticed that there is a great increase in the anodic peak currents at the AuRh nanoparticles modified GCE for the increasing concentrations of AA in pH 7.0 PBS (Fig. 5(A), curve a-g). Here the increasing oxidation peak currents of AA clearly show the electro catalytic activity of the AuRh nanoparticles modified GCE

surface. Here the AuRh nanoparticles modified GCE detects the AA electrooxidation signals in the linear range of 100 to1088 µM. The sensitivity of the AuRh nanoparticles modified GCE for the detection of AA is found to be 0.24 µA μM^{-1}.

3.4. Simultaneous detection of AA and DA at AuRh nanoparticles modified GCE

Simultaneous detection of AA and DA at AuRh nanoparticles modified GCE have been examined using CV (Fig. 5(B)) and LSV (Fig. 6).

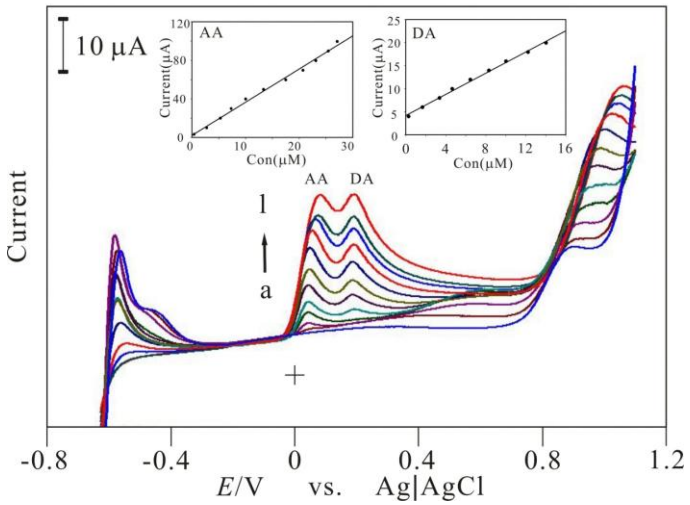

Figure 6. LSVs for the simultaneous detection of AA and DA at AuRh nanoparticles modified GCE in pH 7.0 PBS. AA concentrations were in the range of : (a-l) 0, 3.3, 9.9, 20, 29.9, 39.9, 49.9, 59.8, 69.8, 79.7, 89.7 and 99.6 µM, (a') bare GCE = 99.6 µM. DA concentrations were in the range of : (a-l) 0, 0.67, 2.0, 4, 5, 8, 10, 12, 14, 16, 18, and 19 µM, (a') bare GCE = 19 µM. (scan rate: 0.1 V/s). Inset shows the calibration plot of current vs. concentration plots of AA and DA.

Here the AuRh nanoparticles modified GCE successfully overcomes the fouling effect and shows two well distinguished oxidation peaks for the detection of AA and DA. The anodic oxidation current peaks for the detection of AA and DA were found at 0.03 and 0.18 V at AuRh nanoparticles modified GCE, whereas for the bare GCE it fails to exhibit into two anodic oxidation peaks and showed as a single peak at around 0.22 V. Therefore, a decrease in over potential and the significant enhancement of the anodic oxidation peak current for the detection of AA and DA is achieved at the AuRh nanoparticles modified GCE. This result is a clear indication for the occurrence of electro catalytic oxidation and simultaneous detection of AA and DA at the AuRh nanoparticles modified GCE. Also, the corresponding anodic peak currents of AA and DA were clearly increasing with respect to the increasing concentrations in pH 7.0 PBS. Here the AuRh nanoparticles modified GCE detects the AA and DA electrooxidation signals in the linear ranges of 2.8 to 102 µM and 0.71 to 25.6 µM, respectively. The inset of Fig. 5(B) shows the oxidation peak currents vs. concentration plot for

the electrocatalytic oxidations of AA and DA. The sensitivity of the AA and DA detection at the AuRh nanoparticles modified GCE were found as 0.31 and 6.2 μA μM^{-1}.

Further the simultaneous detection of AA and DA also has been examined using LSV technique (Fig. 6). Here too the proposed AuRh nanoparticles modified GCE exhibits two well defined separate anodic oxidation peaks for AA and DA. The anodic oxidation peaks for AA and DA have been found at 0.04 and 0.18 V. Also, the corresponding oxidation peaks clearly increasing with respect to the increasing concentrations of AA and DA.

Here the AuRh nanoparticles modified GCE detects the AA and DA electrooxidation signals in the linear ranges of 3.3 to 99.6 μM and 0.67 to 19. μM, respectively. The inset of Fig. 6 shows the oxidation peak current vs. concentration plots for the electrocatalytic oxidations of AA and DA. Based on the calibration plot the sensitivity of the proposed electrode for the simultaneous detection of AA and DA has been found as 3.4 and 1.14 μA μM^{-1}.

3.5. Bromate detection at AuRh nanoparticles modified GCE

The detection of bromate has been examined using CV and LSV techniques (Fig. 7(A)and (B)).

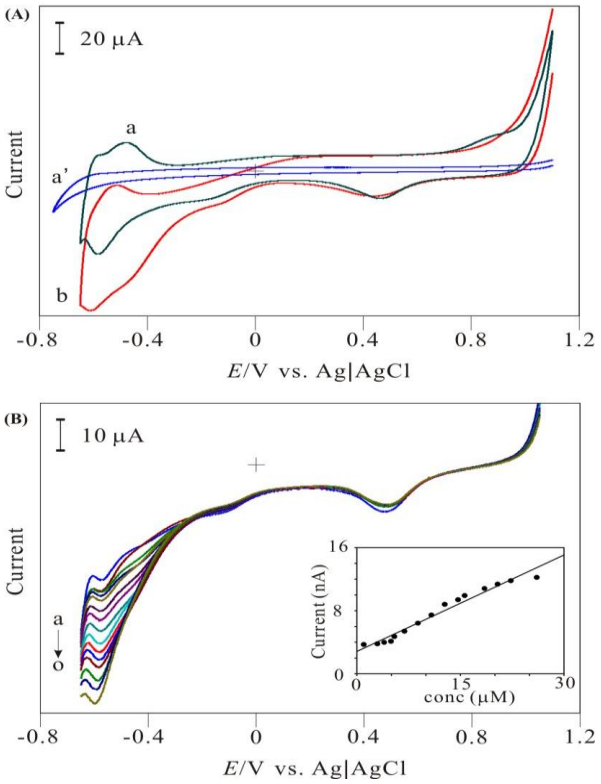

Figure 7. (A) CV response for the bromate detection (18.5 μM) at bare (curve a') and AuRh nanoparticles modified GCE (curve b) in pH 7.0 PBS (curve a: CV response of AuRh nanoparticles modified GCE in pH 7.0 PBS). (B) LSV response of AuRh nanoparticles modified GCE for the detection of bromate in pH 7.0 PBS. Bromate concentrations were in the range of: (a-o) 1, 2.96, 3.95, 4.9, 5.4, 6.8, 8.8, 10.7, 12.7, 14.6, 15.6, 18.4, 20.3, 22.2 and 26 μM, (a') bare GCE = 26 μM (scan rate: 0.1 V/s). Inset shows the calibration plot of reduction current vs. concentration plot of bromate detection.

Here reduction peak for the bromated detection is found at -0.59 V for AuRh nanoparticles modified GCE, whereas for the bare GCE it fails to exhibit reduction peak current for the bromate. This shows that the proposed film modified GCE possess the electrocatalytic activity for the detection of bromate. Further LSV technique employed for the detailed analysis of bromate detection.

Fig 7(B) shows the LSV response of AuRh nanoparticles modified GCE for the detection of bromate in pH 7.0 PBS. Here the cathodic peak current of reduction of bromate (at -0.55 V) detection was clearly increasing at the AuRh nanoparticles modified GCE. Here the AuRh nanoparticles modified GCE detects the bromate reduction signals in the linear range of 1 to 26 µM. Further the inset of Fig. 7(B) shows the reduction peak current vs. concentration plot for the electrocatalytic reduction of bromate detection. The sensitivity of the AuRh nanoparticles modified GCE for bromate detection has been found as 0.40 µA μM^{-1}. All these results clearly shows that the proposed AuRh nanoparticles modified GCE could be employed for the detection of AA, simultaneous detection of AA and DA and bromate in lab and real samples.

4. CONCLUSION

We have attempted to fabricate AuRh nanoparticles using electrochemical deposition method (CV). The proposed method successfully utilized for the fabrication of AuRh nanoparticles modified GCE and ITO. The electrodeposited AuRh nanoparticles modified GCE has been characterized using SEM and AFM techniques. Also, the AuRh nanoparticles modified ITO has been studied using XRD analysis. The proposed film modified GCE successfully employed for the detection of AA and simultaneous detection and determination of AA and DA in pH 7.0 PBS. Also, the AuRh nanoparticles modified GCE successfully shows the reduction peak for bromate in the pH 7.0 PBS. Overall, the proposed nanoparticle film is easy to fabricate and could be employed as the sensor for the detection of AA and DA and bromate detection process and related studies, respectively.

ACKNOWLEDGMENT
This work was supported by grants from National Science Council (NSC) of Taiwan (ROC).

References

1. T. Selvaraju, R. Ramaraj, *J. Electroanal. Chem.*, 585 (2005) 290.
2. J. Luo, P.N. Njoki, D. Mott, L. Wang, C.-J. Zhong, *Langmuir* 22 (2006) 2892.
3. S. Thiagarajan, S.-M. Chen, Talanta 74 (2007) 212.
4. J. Liu, W. Huang, S. Chen, S. Hu, F.Liu, Z. Li, *Int. J. Electrochem. Sci.*, 4 (2009) 1302.
5. G.A. Jorge, J.D. Martínez, M.C. Bullón, D. Sousa, C. U. Navarro, *Port Electrochim. Acta,* 27 (2009) 279.
6. B.R. Sathe, D. B. Shinde, V. K. Pillai, *J. Phys. Chem.* C 113 (2009) 9616.
7. S. Chandraa, K.S. Lokesh, Anja Nicolai, Heinrich Lang, *Anal. Chim. Acta* 632 (2009) 63.
8. H.-B. Pan, C.M. Wai, *J. Phys. Chem.* C 114 (2010) 11364.
9. M. Harada, H. Einaga, *J. Coll. Inter. Sci*., 308 (2007) 568.
10. S. Alayoglu, B. Eichhorn, *J. Am. Chem. Soc*., 130 (2008) 17479.
11. V. Abdelsayed, A. Aljarash, M. S. El-Shall, *Chem. Mater.*, 21 (2009) 2825.

12. J.Y. Park, Y. Zhang, M. Grass, T. Zhang, G.A. Somorjai, *Nano Lett*., 8 (2008) 673.
13. F.H.B. Lima, E.R. Gonzalez, *Applied Catalysis B: Environmental* 79 (2008) 341–346.
14. K.-W. Park, D.-S. Han, Y.-E. Sung, *J. of Power. Sour*., 163 (2006) 82.
15. K. Maeda, D. Lu, K. Teramura, K. Domen, *Energy Environ. Sci*., 3 (2010) 471.
16. S. Reddy, B.E. Kumara Swamy, Umesh Chandra, B.S.Sherigara, H.Jayadevappa, *Int. J. Electrochem. Sci.*, 5 (2010) 10.
17. M.M. Ardakani, H. Rajabi, H. Beitollahi, B.B. Fatemah Mirjalili, A. Akbari, N. Taghavinia, *Int. J. Electrochem. Sci.*, 5 (2010) 147.
18. M. M. Ardakani, R. Arazi, H. Naeimi, *Int. J. Electrochem. Sci.*, 5 (2010) 1773.